Eur. Phys. J. C 23, 275–287 (2002)
Digital Object Identifier (DOI) 10.1007/s100520100878

THE EUROPEAN PHYSICAL JOURNAL C

$B \to \pi\rho$, $\pi\omega$ decays in perturbative QCD approach

C.-D. Lü[1,2,3], M.-Z. Yang[1,2,3]

[1] CCAST (World Laboratory), P.O. Box 8730, Beijing 100080, P.R. China
[2] Institute of High Energy Physics, CAS, P.O. Box 918(4), Beijing 100039, P.R. China*
[3] Physics Department, Hiroshima University, Higashi-Hiroshima 739-8526, Japan

Received: 5 November 2001 /
Published online: 8 February 2002 –

Abstract. We calculate the branching ratios and CP-asymmetries for $B^0 \to \pi^+\rho^-$, $B^0 \to \rho^+\pi^-$, $B^+ \to \rho^+\pi^0$, $B^+ \to \pi^+\rho^0$, $B^0 \to \pi^0\rho^0$, $B^+ \to \pi^+\omega$ and $B^0 \to \pi^0\omega$ decays, in the perturbative QCD approach. In this approach, we calculate non-factorizable and annihilation type contributions, in addition to the usual factorizable contributions. Our result is in agreement with the branching ratio of $B^0/\bar{B}^0 \to \pi^\pm\rho^\mp$, $B^\pm \to \pi^\pm\rho^0$, $\pi^\pm\omega$ measured by the CLEO and BABAR collaborations. We also predict large CP-asymmetries in these decays. These channels are useful to determine the CKM angle ϕ_2.

1 Introduction

The rare decays of the B-mesons are getting more and more interesting, since they are useful for the search of CP-violation and sensitive to new physics. The recent measurement of $B \to \pi\rho$ and $\pi\omega$ decays by the CLEO Collaboration [1] aroused more discussions on these decays [2]. The $B \to \pi\rho$, $\pi\omega$ decays which are helpful for the determination of the Cabbibo–Kobayashi–Maskawa (CKM) unitarity triangle ϕ_2 have been studied in the factorization approach in detail [3,4]. In this paper, we would like to study the $B \to \pi\rho$ and $\pi\omega$ decays in the perturbative QCD approach (PQCD), where we can calculate the non-factorizable contributions as corrections to the usual factorization approach.

In the $B \to \pi\rho$, $\pi\omega$ decays, the B-meson is heavy, sitting at rest. It decays into two light mesons with large momenta. Therefore the light mesons are moving very fast in the rest frame of the B-meson. In this case, the short distance hard process dominates the decay amplitude. The reasons can be ordered as: first, because there are not many resonances near the energy region of the B mass, it is reasonable to assume that the final state interaction is not important in two-body B decays. Second, with the final light mesons moving very fast, there must be a hard gluon to kick the light spectator quark (almost at rest) in the B-meson to form a fast moving pion or light vector meson. So the dominant diagram in this theoretical picture is the one with a hard gluon from the spectator quark connecting with the other quarks in the four quark operator of the weak interaction. There are also soft (soft and collinear) gluon exchanges between the quarks. Summing over those leading soft contributions gives a Sudakov form factor which suppresses the dominance of the soft contribution. This makes the PQCD reliable in calculating the non-leptonic decays. With the Sudakov resummation, we can include the leading double logarithms for all loop diagrams, in association with the soft contribution. Unlike the usual factorization approach, the hard part of the PQCD approach consists of six quarks rather than four. We thus call it the case of six-quark operators or six-quark effective theory. Applying the six-quark effective theory to B-meson decays, we need meson wave functions for the hadronization of quarks into mesons. All the collinear dynamics is included in the meson wave functions.

In this paper, we calculate the $B \to \pi$ and $B \to \rho$ form factors, which are input parameters used in the factorization approach. The form factor calculations can give severe restrictions to the input meson wave functions. We also calculate the non-factorizable contributions and the annihilation type diagrams, which are difficult to calculate in the factorization approach. We found that this type of diagrams gives dominant contributions to the strong phases. The strong phase in this approach can also be calculated directly, without ambiguity. In the next section, we will briefly introduce our method of PQCD. In Sect. 3, we perform the perturbative calculations for all the channels. We give the numerical results and discussions in Sect. 4. Finally Sect. 5 is a short summary.

2 The framework

The three scale PQCD factorization theorem has been developed for non-leptonic heavy meson decays [5]. The factorization formula is given by the typical expression

$$C(t) \times H(x,t) \times \Phi(x)$$

* Mailing address

$$\times \exp\left[-s(P,b) - 2\int_{1/b}^{t} \frac{\mathrm{d}\bar{\mu}}{\bar{\mu}} \gamma_q(\alpha_\mathrm{s}(\bar{\mu}))\right], \qquad (1)$$

where $C(t)$ are the corresponding Wilson coefficients, $\Phi(x)$ are the meson wave functions. The quark anomalous dimension $\gamma_q = -\alpha_\mathrm{s}/\pi$ describes the evolution from scale t to $1/b$.

Non-leptonic heavy meson decays involve three scales: the W-boson mass m_W, at which the matching conditions of the effective Hamiltonian is defined, the typical scale t of a hard sub-amplitude, which reflects the dynamics of heavy quark decays, and the factorization scale $1/b$, with b the conjugate variable of the parton transverse momenta. The dynamics below the $1/b$ scale is regarded as being completely non-perturbative, and can be parameterized into meson wave functions. Above the scale $1/b$, PQCD is reliable and radiative corrections produce two types of large logarithms: $\ln(m_W/t)$ and $\ln(tb)$. The former are summed by the renormalization group equations to give the leading logarithm evolution from m_W to the t scale contained in the Wilson coefficients $C(t)$, while the latter are summed to give the evolution from the t scale down to $1/b$, shown as the last factor in (1).

There exist also double logarithms $\ln^2(Pb)$ from the overlap of collinear and soft divergences, P being the dominant light-cone component of a meson momentum. The resummation of these double logarithms leads to a Sudakov form factor $\exp[-s(P,b)]$, which suppresses the long distance contributions in the large b region, and vanishes as $b > 1/\Lambda_\mathrm{QCD}$. This factor improves the applicability of PQCD. For the detailed derivation of the Sudakov form factors, see [6,7]. Since all logarithm corrections have been summed by renormalization group equations, the above factorization formula does not depend on the renormalization scale μ.

With all the large logarithms resummed, the remaining finite contributions are absorbed into a hard sub-amplitude $H(x,t)$. The $H(x,t)$ is calculated perturbatively using the four quark operators together with the spectator quark, connected by a hard gluon. When the end-point region ($x \to 0,1$) of the wave function is important for the hard amplitude, the corresponding large double logarithms $\alpha_\mathrm{s} \ln^2 x$ shall appear in the hard amplitude $H(x,t)$, which should be resummed to give a jet function $S_t(x)$. This technique is the so-called threshold resummation [8]. The threshold resummation form factor $S_t(x)$ vanishes as $x \to 0,1$, which effectively suppresses the end-point behavior of the hard amplitude. This suppression will become important when the meson wave function remains constant at the end-point region. For example, the twist-3 wave functions ϕ_π^P and ϕ_π^t are such kinds of wave functions; they can be found in the numerical section of this paper. The typical scale t in the hard sub-amplitude is around $(\Lambda M_B)^{1/2}$. It is chosen as the maximum value of those scales which appear in the six-quark action. This is to diminish the α_s^2 corrections to the six-quark amplitude. The expressions of the scale t in different sub-amplitudes will be derived in the next section and the formula is shown in the appendix.

2.1 Wilson coefficients

First we begin with the weak effective Hamiltonian H_eff for the $\Delta B = 1$ transitions:

$$\mathcal{H}_\mathrm{eff} = \frac{G_F}{\sqrt{2}} \left[V_{ub}V_{ud}^* \left(C_1 O_1^u + C_2 O_2^u\right) - V_{tb}V_{td}^* \sum_{i=3}^{10} C_i\, O_i\right]. \qquad (2)$$

We specify below the operators in $\mathcal{H}_\mathrm{eff}$ for $b \to d$:

$$\begin{aligned}
O_1^u &= \bar{d}_\alpha \gamma^\mu L u_\beta \cdot \bar{u}_\beta \gamma_\mu L b_\alpha,\\
O_2^u &= \bar{d}_\alpha \gamma^\mu L u_\alpha \cdot \bar{u}_\beta \gamma_\mu L b_\beta,\\
O_3 &= \bar{d}_\alpha \gamma^\mu L b_\alpha \cdot \sum_{q'} \bar{q}'_\beta \gamma_\mu L q'_\beta,\\
O_4 &= \bar{d}_\alpha \gamma^\mu L b_\beta \cdot \sum_{q'} \bar{q}'_\beta \gamma_\mu L q'_\alpha,\\
O_5 &= \bar{d}_\alpha \gamma^\mu L b_\alpha \cdot \sum_{q'} \bar{q}'_\beta \gamma_\mu R q'_\beta,\\
O_6 &= \bar{d}_\alpha \gamma^\mu L b_\beta \cdot \sum_{q'} \bar{q}'_\beta \gamma_\mu R q'_\alpha,\\
O_7 &= \frac{3}{2}\bar{d}_\alpha \gamma^\mu L b_\alpha \cdot \sum_{q'} e_{q'} \bar{q}'_\beta \gamma_\mu R q'_\beta,\\
O_8 &= \frac{3}{2}\bar{d}_\alpha \gamma^\mu L b_\beta \cdot \sum_{q'} e_{q'} \bar{q}'_\beta \gamma_\mu R q'_\alpha,\\
O_9 &= \frac{3}{2}\bar{d}_\alpha \gamma^\mu L b_\alpha \cdot \sum_{q'} e_{q'} \bar{q}'_\beta \gamma_\mu L q'_\beta,\\
O_{10} &= \frac{3}{2}\bar{d}_\alpha \gamma^\mu L b_\beta \cdot \sum_{q'} e_{q'} \bar{q}'_\beta \gamma_\mu L q'_\alpha. \qquad (3)
\end{aligned}$$

Here α and β are the $SU(3)$ color indices; L and R are the left- and right-handed projection operators with $L = (1-\gamma_5)$, $R = (1+\gamma_5)$. The sum over q' runs over the quark fields that are active at the scale $\mu = O(m_b)$, i.e., $(q' \epsilon \{u,d,s,c,b\})$.

The PQCD approach works well for the leading twist approximation and leading double logarithm summation. For the Wilson coefficients, we will also use the leading logarithm summation for the QCD corrections, although the next-to-leading order calculations already exists in the literature [9]. This is the consistent way to cancel the explicit μ dependence in the theoretical formulae.

If the scale $m_b < t < m_W$, then we evaluate the Wilson coefficients at a t scale using the leading logarithm running equations [9] in Appendix B of [10]. In numerical calculations, we use $\alpha_\mathrm{s} = 4\pi/[\beta_1 \ln(t^2/\Lambda_\mathrm{QCD}^{(5)\,2})]$ which is the leading order expression with $\Lambda_\mathrm{QCD}^{(5)} = 193\,\mathrm{MeV}$, derived for $\Lambda_\mathrm{QCD}^{(4)} = 250\,\mathrm{MeV}$. Here $\beta_1 = (33-2n_f)/12$, with the appropriate number of active quarks n_f. $n_f = 5$ when the scale t is larger than m_b.

If the scale $t < m_b$, then we evaluate the Wilson coefficients at the t scale using the formulae in Appendix C of [10] for four active quarks ($n_f = 4$) (again in leading logarithm approximation).

2.2 Wave functions

In the resummation procedure, the B-meson is treated as a heavy-light system. In general, the B-meson light-cone matrix element can be decomposed as [11,12]

$$\int_0^1 \frac{\mathrm{d}^4 z}{(2\pi)^4} \mathrm{e}^{\mathrm{i}\boldsymbol{k_1}\cdot z} \langle 0|\bar{b}_\alpha(0) d_\beta(z)|B(p_B)\rangle = -\frac{\mathrm{i}}{\sqrt{2N_c}} \left\{ (\not{p}_B + m_B)\gamma_5 \times \left[\phi_B(\boldsymbol{k}_1) - \frac{\not{n}- \not{v}}{\sqrt{2}} \bar{\phi}_B(\boldsymbol{k}_1)\right] \right\}_{\beta\alpha}, \quad (4)$$

where $n = (1, 0, \mathbf{0_T})$, and $v = (0, 1, \mathbf{0_T})$ are the unit vectors pointing to the plus and minus directions, respectively. From the above equation, one can see that there are two Lorentz structures in the B-meson distribution amplitudes. They obey the following normalization conditions:

$$\int \frac{\mathrm{d}^4 k_1}{(2\pi)^4} \phi_B(\boldsymbol{k}_1) = \frac{f_B}{2\sqrt{2N_c}}, \quad \int \frac{\mathrm{d}^4 k_1}{(2\pi)^4} \bar{\phi}_B(\boldsymbol{k}_1) = 0. \quad (5)$$

In general, one should consider both these two Lorentz structures in calculations of B-meson decays. However, it can be argued that the contribution of $\bar{\phi}_B$ is numerically small [13]; thus its contribution can be neglected. Therefore, we only consider the contribution of the Lorentz structure

$$\Phi_B = \frac{1}{\sqrt{2N_c}} (\not{p}_B + m_B)\gamma_5 \phi_B(\boldsymbol{k}_1) \quad (6)$$

in our calculation. We keep the same input as in the other calculations in this direction [10,13,14] and it is also easier for comparing with other approaches [12,15]. Throughout this paper, we use the light-cone coordinates to write the four momentum as $(k_1^+, k_1^-, k_1^\perp)$. In the next section, we will see that the hard part is always independent of one of the k_1^+ and/or k_1^-, if we make some approximations. The B-meson wave function is then a function of the variables k_1^- (or k_1^+) and $k_1^\perp$,

$$\phi_B(k_1^-, k_1^\perp) = \int \mathrm{d}k_1^+ \phi(k_1^+, k_1^-, k_1^\perp). \quad (7)$$

The π-meson is treated as a light-light system. In the B-meson rest frame, the pion is moving very fast, and one of the k_1^+ or k_1^- is zero which depends on the definition of the z axis. We consider a pion moving in the minus direction in this paper. The pion distribution amplitude is defined by [16]

$$\langle \pi^-(P)|\bar{d}_\alpha(z) u_\beta(0)|0\rangle = \frac{\mathrm{i}}{\sqrt{2N_c}} \int_0^1 dx \mathrm{e}^{\mathrm{i}xP\cdot z} \left[\gamma_5 \not{P}\phi_\pi(x) + m_0\gamma_5\phi_P(x) - m_0\sigma^{\mu\nu}\gamma_5 P_\mu z_\nu \frac{\phi_\sigma(x)}{6}\right]_{\beta\alpha}. \quad (8)$$

For the first and second term in the above equation, we can easily get the projector of the distribution amplitude in the momentum space. However, for the third term we should make some effort to transfer it into the momentum space. By using integration by parts for the third term, after a few steps, (8) can be finally changed to

$$\langle \pi^-(P)|\bar{d}_\alpha(z) u_\beta(0)|0\rangle = \frac{\mathrm{i}}{\sqrt{2N_c}} \int_0^1 dx \mathrm{e}^{\mathrm{i}xP\cdot z} \Big[\gamma_5 \not{P}\phi_\pi(x) + m_0\gamma_5\phi_P(x) + m_0[\gamma_5(\not{v}\not{n} - 1)]\phi_\pi^t(x)\Big]_{\beta\alpha}, \quad (9)$$

where $\phi_\pi^t(x) = (1/6)(d/x)\phi_\sigma(x)$, and the vector v is parallel to the π-meson momentum p_π. $m_0 = m_\pi^2/(m_u + m_d)$ is a scale characterized by chiral perturbation theory. In $B \to \pi\rho$ decays, the ρ-meson is only longitudinally polarized. We only consider its wave function in longitudinal polarization [13,17]:

$$\langle \rho^-(P, \epsilon_L)|\bar{d}_\alpha(z) u_\beta(0)|0\rangle = \frac{1}{\sqrt{2N_c}} \int_0^1 dx \mathrm{e}^{\mathrm{i}xP\cdot z} \Big\{ \not{\epsilon}\big[\not{p}_\rho \phi_\rho^t(x) + m_\rho \phi_\rho(x)\big] + m_\rho \phi_\rho^s(x)\Big\}. \quad (10)$$

The second term in the above equation is the leading twist wave function (twist-2), while the first and third terms are sub-leading twist (twist-3) wave function.

The transverse momentum $k^\perp$ is usually conveniently converted to the b parameter by a Fourier transformation. The initial conditions of $\phi_i(x)$, $i = B$, π, are of non-perturbative origin, satisfying the normalization

$$\int_0^1 \phi_i(x, b = 0)\mathrm{d}x = \frac{1}{2\sqrt{6}} f_i, \quad (11)$$

with f_i the meson decay constant.

3 Perturbative calculations

In the previous section we have discussed the wave functions and Wilson coefficients of the factorization formula in (1). In this section, we will calculate the hard part $H(t)$. This part involves the four quark operators and the necessary hard gluon connecting the four quark operator and the spectator quark. Since the final results are expressed as integrations of the distribution function variables, we will show the whole amplitude for each diagram including wave functions.

Similar to the $B \to \pi\pi$ decays [10], there are 8 types of diagrams contributing to the $B \to \pi\rho$ decays, which are shown in Fig. 1. Let us first calculate the usual factorizable diagrams a and b. The operators O_1, O_2, O_3, O_4, O_9, and O_{10} are $(V - A)(V - A)$ currents, and the sum of their amplitudes is given by

$$F_e = 8\sqrt{2}\pi C_F G_\mathrm{F} f_\rho m_\rho m_B^2 (\epsilon \cdot p_\pi)$$

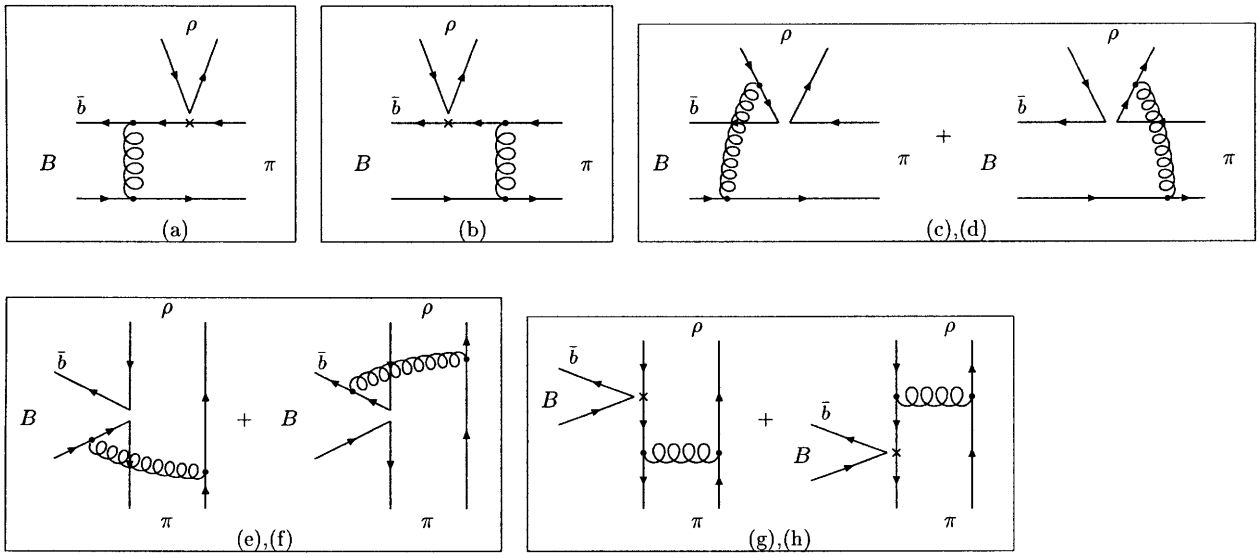

Fig. 1a–h. Diagrams contributing to the $B \to \pi\rho$ decays (diagram **a** and **b** contribute to the $B \to \pi$ form factor)

$$
\begin{aligned}
&\times \int_0^1 \mathrm{d}x_1\mathrm{d}x_2 \int_0^\infty b_1\mathrm{d}b_1 b_2\mathrm{d}b_2 \phi_B(x_1,b_1) \\
&\times \Bigg\{ \Big[(1+x_2)\phi_\pi^A(x_2,b_2) \\
&+ r_\pi(1-2x_2)\left(\phi_\pi^P(x_2,b_2)+\phi_\pi^\sigma(x_2,b_2)\right)\Big]\alpha_\mathrm{s}(t_e^1) \\
&\times h_e(x_1,x_2,b_1,b_2)\exp[-S_{ab}(t_e^1)] \\
&+ 2r_\pi\phi_\pi^P(x_2,b_2)\alpha_\mathrm{s}(t_e^2)h_e(x_2,x_1,b_2,b_1) \\
&\times \exp[-S_{ab}(t_e^2)]\Bigg\}, \qquad (12)
\end{aligned}
$$

where $r_\pi = m_0/m_B = m_\pi^2/[m_B(m_u+m_d)]$; $C_F = 4/3$ is a color factor. The function h_e, the scales t_e^i and the Sudakov factors S_{ab} are displayed in the appendix. In the above equation, we do not include the Wilson coefficients of the corresponding operators, which are process dependent. They will be shown later in this section for different decay channels. The diagrams in Fig. 1a,b are also the diagrams for the $B \to \pi$ form factor $F_1^{B\to\pi}$. Therefore we can extract $F_1^{B\to\pi}$ from (12). We have

$$
F_1^{B\to\pi}(q^2=0) = \frac{F_e}{\sqrt{2}G_\mathrm{F} f_\rho m_\rho(\epsilon\cdot p_\pi)}. \qquad (13)
$$

The operators O_5, O_6, O_7, and O_8 have the structure of $(V-A)(V+A)$. In some decay channels, some of these operators contribute to the decay amplitude in a factorizable way. Since only the vector part of the $(V+A)$ current contributes to the vector meson production,

$$
\langle\pi|V-A|B\rangle\langle\rho|V+A|0\rangle = \langle\pi|V-A|B\rangle\langle\rho|V-A|0\rangle, \quad (14)
$$

the result of these operators is the same as (12). In some other cases, we need to do a Fierz transformation for these operators to get the right color structure for the factorization to work. In this case, we get $(S-P)(S+P)$ operators from $(V-A)(V+A)$ ones. Because neither the scalar nor the pseudo-scalar density give contributions to the vector meson production, i.e. $\langle\rho|S+P|0\rangle = 0$, we get

$$
F_e^P = 0. \qquad (15)
$$

For the non-factorizable diagrams c and d, all three meson wave functions are involved. The integration of b_3 can be performed easily using the δ function $\delta(b_3-b_1)$, leaving only the integration of b_1 and b_2. For the $(V-A)(V-A)$ operators the result is

$$
\begin{aligned}
M_e = &-\frac{32}{3}\sqrt{3}\pi C_F G_\mathrm{F} m_\rho m_B^2(\epsilon\cdot p_\pi) \\
&\times \int_0^1 \mathrm{d}x_1\mathrm{d}x_2\mathrm{d}x_3 \int_0^\infty b_1\mathrm{d}b_1 b_2\mathrm{d}b_2\phi_B(x_1,b_1) \\
&\times x_2\left[\phi_\pi^A(x_2,b_1) - 2r_\pi\phi_\pi^\sigma(x_2,b_1)\right] \\
&\times \phi_\rho(x_3,b_2)h_d(x_1,x_2,x_3,b_1,b_2)\exp[-S_{cd}(t_d)]. \qquad (16)
\end{aligned}
$$

For the $(V-A)(V+A)$ operators the formula is different:

$$
\begin{aligned}
M_e^P = &\frac{64}{3}\sqrt{3}\pi C_F G_\mathrm{F} m_\rho^2 m_B(\epsilon\cdot p_\pi) \\
&\times \int_0^1 \mathrm{d}x_1\mathrm{d}x_2\mathrm{d}x_3 \int_0^\infty b_1\mathrm{d}b_1 b_2\mathrm{d}b_2\phi_B(x_1,b_1) \\
&\times \Big\{ r_\pi(x_3-x_2) \\
&\times \left[\phi_\pi^P(x_2,b_1)\phi_\rho^t(x_3,b_2) + \phi_\pi^\sigma(x_2,b_1)\phi_\rho^s(x_3,b_2)\right] \\
&- r_\pi(x_2+x_3) \\
&\times \left[\phi_\pi^P(x_2,b_1)\phi_\rho^s(x_3,b_2) + \phi_\pi^\sigma(x_2,b_1)\phi_\rho^t(x_3,b_2)\right] \\
&+ x_3\phi_\pi^A(x_2,b_1)\left[\phi_\rho^t(x_3,b_2) - \phi_\rho^s(x_3,b_2)\right]\Big\} \\
&\times h_d(x_1,x_2,x_3,b_1,b_2)\exp[-S_{cd}(t_d)]. \qquad (17)
\end{aligned}
$$

Comparing with the expression of M_e in (16), the $(V-A)(V+A)$ type result M_e^P is suppressed by m_ρ/m_B.

For the non-factorizable annihilation diagrams e and f, again all three wave functions are involved. The integration of b_3 can be performed easily using the δ function $\delta(b_3 - b_2)$. Here we have two kinds of contribution, which are different. M_a is the contribution containing the operator of type $(V-A)(V-A)$, and M_a^P is the contribution containing the operator of type $(V-A)(V+A)$:

$$\begin{aligned}
M_a &= \frac{32}{3}\sqrt{3}\pi C_F G_{\rm F} m_\rho m_B^2 (\epsilon\cdot p_\pi) \\
&\times \int_0^1 {\rm d}x_1{\rm d}x_2{\rm d}x_3 \int_0^\infty b_1{\rm d}b_1 b_2{\rm d}b_2 \phi_B(x_1,b_1) \\
&\times \Bigg\{ \Big[x_2\phi_\pi^A(x_2,b_2)\phi_\rho(x_3,b_2) + r_\pi r_\rho(x_2-x_3) \\
&\times \left(\phi_\pi^P(x_2,b_2)\phi_\rho^t(x_3,b_2) + \phi_\pi^\sigma(x_2,b_2)\phi_\rho^s(x_3,b_2)\right) \\
&+ r_\pi r_\rho(x_2+x_3) \\
&\times \left(\phi_\pi^\sigma(x_2,b_2)\phi_\rho^t(x_3,b_2) + \phi_\pi^P(x_2,b_2)\phi_\rho^s(x_3,b_2)\right)\Big] \\
&\times h_f^1(x_1,x_2,x_3,b_1,b_2)\exp[-S_{ef}(t_f^1)] \\
&- \Big[x_3\phi_\pi^A(x_2,b_2)\phi_\rho(x_3,b_2) + r_\pi r_\rho(x_3-x_2) \\
&\times \left(\phi_\pi^P(x_2,b_2)\phi_\rho^t(x_3,b_2) + \phi_\pi^\sigma(x_2,b_2)\phi_\rho^s(x_3,b_2)\right) \\
&+ r_\pi r_\rho(2+x_2+x_3)\phi_\pi^P(x_2,b_2)\phi_\rho^s(x_3,b_2) \\
&- r_\pi r_\rho(2-x_2-x_3)\phi_\pi^\sigma(x_2,b_2)\phi_\rho^t(x_3,b_2)\Big] \\
&\times h_f^2(x_1,x_2,x_3,b_1,b_2)\exp[-S_{ef}(t_f^2)]\Bigg\}, \qquad (18)
\end{aligned}$$

$$\begin{aligned}
M_a^P &= -\frac{32}{3}\sqrt{3}\pi C_F G_{\rm F} m_\rho m_B^2 (\epsilon\cdot p_\pi) \\
&\times \int_0^1 {\rm d}x_1{\rm d}x_2{\rm d}x_3 \int_0^\infty b_1{\rm d}b_1 b_2{\rm d}b_2 \phi_B(x_1,b_1) \\
&\times \Bigg\{ \Big[x_2 r_\pi \phi_\rho(x_3,b_2)\left(\phi_\pi^P(x_2,b_2) + \phi_\pi^\sigma(x_2,b_2)\right) \\
&- x_3 r_\rho \phi_\pi^A(x_2,b_2)\left(\phi_\rho^t(x_3,b_2) + \phi_\rho^s(x_3,b_2)\right)\Big] \\
&\times h_f^1(x_1,x_2,x_3,b_1,b_2)\exp[-S_{ef}(t_f^1)] \\
&+ \Big[(2-x_2) r_\pi \phi_\rho(x_3,b_2)\left(\phi_\pi^P(x_2,b_2) + \phi_\pi^\sigma(x_2,b_2)\right) \\
&- r_\rho(2-x_3)\phi_\pi^A(x_2,b_2)\left(\phi_\rho^t(x_3,b_2) + \phi_\rho^s(x_3,b_2)\right)\Big] \\
&\times h_f^2(x_1,x_2,x_3,b_1,b_2)\exp[-S_{ef}(t_f^2)]\Bigg\}, \qquad (19)
\end{aligned}$$

where $r_\rho = m_\rho/m_B$. The factorizable annihilation diagrams g and h involve only the π and ρ wave functions. There are also two kinds of decay amplitudes for these two diagrams. F_a is for $(V-A)(V-A)$ type operators, and F_a^P is for $(S-P)(S+P)$ type operators:

$$\begin{aligned}
F_a &= 8\sqrt{2}C_F G_{\rm F}\pi f_B m_\rho m_B^2 (\epsilon\cdot p_\pi) \\
&\times \int_0^1 {\rm d}x_1{\rm d}x_2 \int_0^\infty b_1{\rm d}b_1 b_2{\rm d}b_2 \\
&\times \Bigg\{ \Big[x_2\phi_\pi^A(x_1,b_1)\phi_\rho(x_2,b_2) \\
&- 2(1-x_2) r_\pi r_\rho \phi_\pi^P(x_1,b_1)\phi_\rho^t(x_2,b_2) \\
&+ 2(1+x_2) r_\pi r_\rho \phi_\pi^P(x_1,b_1)\phi_\rho^s(x_2,b_2)\Big] \\
&\times \alpha_{\rm s}(t_e^1) h_a(x_2,x_1,b_2,b_1)\exp[-S_{gh}(t_e^1)] \\
&- \Big[x_1\phi_\pi^A(x_1,b_1)\phi_\rho(x_2,b_2) \\
&+ 2(1+x_1) r_\pi r_\rho \phi_\pi^P(x_1,b_1)\phi_\rho^s(x_2,b_2) \\
&- 2(1-x_1) r_\pi r_\rho \phi_\pi^\sigma(x_1,b_1)\phi_\rho^s(x_2,b_2)\Big] \\
&\times \alpha_{\rm s}(t_e^2) h_a(x_1,x_2,b_1,b_2)\exp[-S_{gh}(t_e^2)]\Bigg\}, \qquad (20)
\end{aligned}$$

$$\begin{aligned}
F_a^P &= 16\sqrt{2}C_F G_{\rm F}\pi f_B m_\rho m_B^2 (\epsilon\cdot p_\pi) \\
&\times \int_0^1 {\rm d}x_1{\rm d}x_2 \int_0^\infty b_1{\rm d}b_1 b_2{\rm d}b_2 \\
&\times \Bigg\{ \Big[2r_\pi\phi_\pi^P(x_1,b_1)\phi_\rho(x_2,b_2) + x_2 r_\rho \phi_\pi^A(x_1,b_1) \\
&\times \left(\phi_\rho^s(x_2,b_2) - \phi_\rho^t(x_2,b_2)\right)\Big] \\
&\times \alpha_{\rm s}(t_e^1) h_a(x_2,x_1,b_2,b_1)\exp[-S_{gh}(t_e^1)] \\
&+ \Big[x_1 r_\pi \left(\phi_\pi^P(x_1,b_1) - \phi_\pi^\sigma(x_1,b_1)\right)\phi_\rho(x_2,b_2) \\
&+ 2r_\rho\phi_\pi^A(x_1,b_1)\phi_\rho^s(x_2,b_2)\Big] \\
&\times \alpha_{\rm s}(t_e^2) h_a(x_1,x_2,b_1,b_2)\exp[-S_{gh}(t_e^2)]\Bigg\}, \qquad (21)
\end{aligned}$$

In the above equations, we have used the assumption that $x_1 \ll x_2, x_3$. Since the light quark momentum fraction x_1 in the B-meson is peaked at the small x_1 region, while the quark momentum fraction x_2 of the pion is peaked around 0.5, this is not a bad approximation. The numerical results also show that this approximation makes very little difference in the final result. After using this approximation, all the diagrams are functions of $k_1^- = x_1 m_B/(2^{1/2})$ of the B-meson only, independent of the variable k_1^+. Therefore the integration of (7) is performed safely.

If we exchange the π and ρ in Fig. 1, the result will be different for some diagrams because this will switch the dominant contribution from the $B \to \pi$ form factor to the $B \to \rho$ form factor. The new diagrams are shown in Fig. 2. Inserting $(V-A)(V-A)$ operators, the corresponding amplitude for Fig. 2a,b is

$$\begin{aligned}
F_{e\rho} &= 8\sqrt{2}\pi C_F G_{\rm F} f_\pi m_\rho m_B^2 (\epsilon\cdot p_\pi) \qquad (22) \\
&\times \int_0^1 {\rm d}x_1{\rm d}x_2 \int_0^\infty b_1{\rm d}b_1 b_2{\rm d}b_2 \phi_B(x_1,b_1) \\
&\times \Bigg\{ \Big[(1+x_2)\phi_\rho(x_2,b_2) \\
&+ (1-2x_2) r_\rho \left(\phi_\rho^t(x_2,b_2) + \phi_\rho^s(x_2,b_2)\right)\Big]
\end{aligned}$$

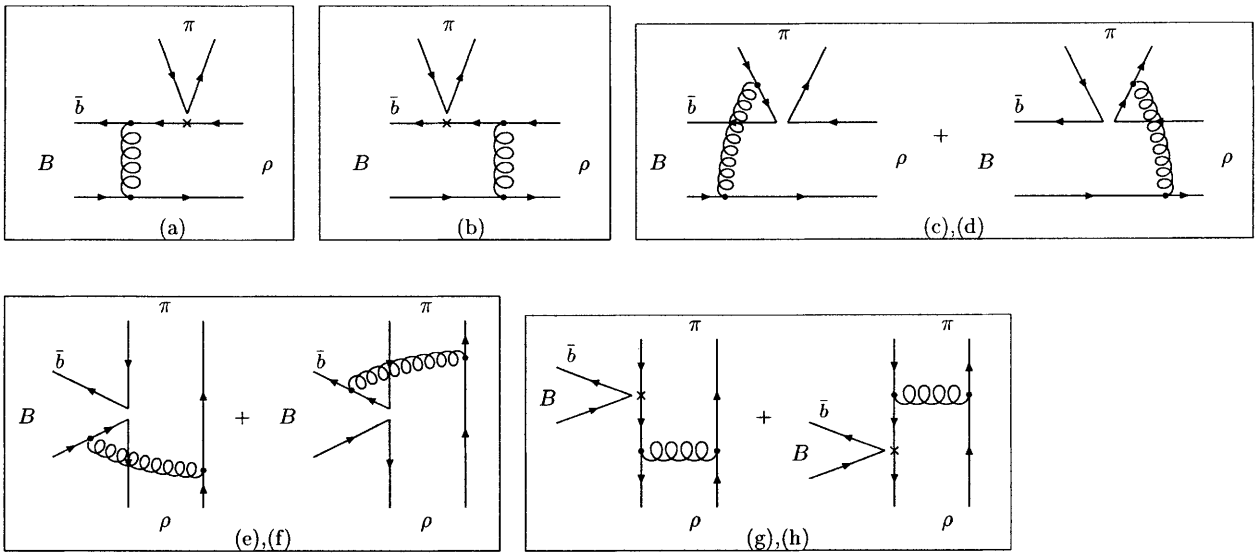

Fig. 2a–h. Diagrams contributing to the $B \to \pi\rho$ decays (diagram **a** and **b** contribute to the $B \to \rho$ form factor $A_0^{B\to\rho}$)

$$\times \alpha_{\rm s}(t_e^1) h_e(x_1, x_2, b_1, b_2) \exp[-S_{ab}(t_e^1)]$$
$$+ 2r_\rho \phi_\rho^s(x_2, b_2) \alpha_{\rm s}(t_e^2) h_e(x_2, x_1, b_2, b_1) \exp[-S_{ab}(t_e^2)] \Big\}.$$

These two diagrams are also responsible for the calculation of the $B \to \rho$ form factors. The form factor relative to the $B \to \pi\rho$ decays is $A_0^{B\to\rho}$, which can be extracted from (22):

$$A_0^{B\to\rho}(q^2 = 0) = \frac{F_{e\rho}}{\sqrt{2} G_{\rm F} f_\pi m_\rho (\epsilon \cdot p_\pi)}. \tag{23}$$

For $(V-A)(V+A)$ operators, Fig. 2a,b give

$$\begin{aligned} F_{e\rho}^P = & -16\sqrt{2}\pi C_F G_{\rm F} f_\pi m_\rho r_\pi m_B^2 (\epsilon \cdot p_\pi) \\ & \times \int_0^1 {\rm d}x_1 {\rm d}x_2 \int_0^\infty b_1 {\rm d}b_1 b_2 {\rm d}b_2 \phi_B(x_1, b_1) \\ & \times \Big\{ \Big[\phi_\rho(x_2, b_2) - r_\rho x_2 \phi_\rho^t(x_2, b_2) \\ & + (2 + x_2) r_\rho \phi_\rho^s(x_2, b_2) \Big] \\ & \times \alpha_{\rm s}(t_e^1) h_e(x_1, x_2, b_1, b_2) \exp[-S_{ab}(t_e^1)] \\ & + \big[x_1 \phi_\rho(x_2, b_2) + 2 r_\rho \phi_\rho^s(x_2, b_2) \big] \\ & \times \alpha_{\rm s}(t_e^2) h_e(x_2, x_1, b_2, b_1) \exp[-S_{ab}(t_e^2)] \Big\}. \end{aligned} \tag{24}$$

For the non-factorizable diagrams in Fig. 2c,d the result is

$$\begin{aligned} M_{e\rho} = & -\frac{32}{3}\sqrt{3}\pi C_F G_{\rm F} m_\rho m_B^2 (\epsilon \cdot p_\pi) \\ & \times \int_0^1 {\rm d}x_1 {\rm d}x_2 {\rm d}x_3 \int_0^\infty b_1 {\rm d}b_1 b_2 {\rm d}b_2 \phi_B(x_1, b_1) \\ & \times x_2 \left[\phi_\rho(x_2, b_2) - 2 r_\rho \phi_\rho^t(x_2, b_2) \right] \\ & \times \phi_\pi^A(x_3, b_1) h_d(x_1, x_2, x_3, b_1, b_2) \\ & \times \exp[-S_{cd}(t_d)]. \end{aligned} \tag{25}$$

For the non-factorizable annihilation diagrams e and f, we have $M_{a\rho}$ for $(V-A)(V-A)$ operators and $M_{a\rho}^P$ for $(V-A)(V+A)$ operators.

$$\begin{aligned} M_{a\rho} = & \frac{32}{3}\sqrt{3}\pi C_F G_{\rm F} m_\rho m_B^2 (\epsilon \cdot p_\pi) \\ & \times \int_0^1 {\rm d}x_1 {\rm d}x_2 {\rm d}x_3 \int_0^\infty b_1 {\rm d}b_1 b_2 {\rm d}b_2 \phi_B(x_1, b_1) \\ & \times \Big\{ \exp[-S_{ef}(t_f^1)] \\ & \times \Big[x_2 \phi_\pi^A(x_3, b_2) \phi_\rho(x_2, b_2) + r_\pi r_\rho (x_2 - x_3) \\ & \times \big(\phi_\pi^P(x_3, b_2) \phi_\rho^t(x_2, b_2) + \phi_\pi^\sigma(x_3, b_2) \phi_\rho^s(x_2, b_2) \big) \\ & + r_\pi r_\rho (x_2 + x_3) \Big(\phi_\pi^\sigma(x_3, b_2) \phi_\rho^t(x_2, b_2) \\ & + \phi_\pi^P(x_3, b_2) \phi_\rho^s(x_2, b_2) \Big) \Big] h_f^1(x_1, x_2, x_3, b_1, b_2) \\ & - \Big[x_3 \phi_\pi^A(x_3, b_2) \phi_\rho(x_2, b_2) + r_\pi r_\rho (x_3 - x_2) \\ & \times \big(\phi_\pi^P(x_3, b_2) \phi_\rho^t(x_2, b_2) + \phi_\pi^\sigma(x_3, b_2) \phi_\rho^s(x_2, b_2) \big) \\ & - r_\pi r_\rho (2 - x_2 - x_3) \phi_\pi^\sigma(x_3, b_2) \phi_\rho^t(x_2, b_2) \\ & + r_\pi r_\rho (2 + x_2 + x_3) \phi_\pi^P(x_3, b_2) \phi_\rho^s(x_2, b_2) \Big] \\ & \times h_f^2(x_1, x_2, x_3, b_1, b_2) \exp[-S_{ef}(t_f^2)] \Big\}, \end{aligned} \tag{26}$$

$$M_{a\rho}^P = M_a^P. \tag{27}$$

For the factorizable annihilation diagrams g and h

$$F_{a\rho} = -F_a, \tag{28}$$
$$F_{a\rho}^P = -F_a^P, \tag{29}$$

If the ρ-meson is replaced by the ω-meson in Figs. 1 and 2, the formulas will be the same, except for replacing f_ρ by f_ω and ϕ_ρ by ϕ_ω.

In the language of the above matrix elements for different diagrams (12)–(29), the decay amplitude for $B^0 \to \pi^+\rho^-$ can be written

$$\begin{aligned}
\mathcal{M}(B^0 \to \pi^+\rho^-) &= F_{e\rho}\left[\xi_u\left(\frac{1}{3}C_1 + C_2\right)\right. \\
&\left. - \xi_t\left(C_4 + \frac{1}{3}C_3 + C_{10} + \frac{1}{3}C_9\right)\right] \\
&-F^P_{e\rho}\xi_t\left[C_6 + \frac{1}{3}C_5 + C_8 + \frac{1}{3}C_7\right] \\
&+M_{e\rho}\left[\xi_u C_1 - \xi_t(C_3 + C_9)\right] \\
&+M_a\left[\xi_u C_2 - \xi_t\left(C_4 - C_6 + \frac{1}{2}C_8 + C_{10}\right)\right] \\
&-M_{a\rho}\xi_t\left[C_3 + C_4 - C_6 - C_8 - \frac{1}{2}C_9 - \frac{1}{2}C_{10}\right] \\
&-M^P_{a\rho}\xi_t\left[C_5 - \frac{1}{2}C_7\right] \;+\; F_a\left[\xi_u\left(C_1 + \frac{1}{3}C_2\right)\right. \\
&\left. -\xi_t\left(-\frac{1}{3}C_3 - C_4 - \frac{3}{2}C_7 - \frac{1}{2}C_8 + \frac{5}{3}C_9 + C_{10}\right)\right] \\
&+F^P_a\xi_t\left[\frac{1}{3}C_5 + C_6 - \frac{1}{6}C_7 - \frac{1}{2}C_8\right], \qquad (30)
\end{aligned}$$

where $\xi_u = V^*_{ub}V_{ud}$, $\xi_t = V^*_{tb}V_{td}$. The $C_i's$ should be calculated at the appropriate scale t using the equations in the appendices of [10]. The decay amplitude of the charge conjugate decay channel $\overline{B}^0 \to \rho^+\pi^-$ is the same as (30) except replacing the CKM matrix elements ξ_u to ξ^*_u and ξ_t to ξ^*_t under the definition of charge conjugation $C|B^0\rangle = -|\overline{B}^0\rangle$. We have

$$\begin{aligned}
\mathcal{M}(B^0 \to \rho^+\pi^-) &= F_e\left[\xi_u\left(\frac{1}{3}C_1 + C_2\right)\right. \\
&\left. - \xi_t\left(C_4 + \frac{1}{3}C_3 + C_{10} + \frac{1}{3}C_9\right)\right] \\
&+M_e\left[\xi_u C_1 - \xi_t(C_3 + C_9)\right] - M^P_e\xi_t[C_5 + C_7] \\
&+M_{a\rho}\left[\xi_u C_2 - \xi_t\left(C_4 - C_6 + \frac{1}{2}C_8 + C_{10}\right)\right] \\
&-M_a\xi_t\left[C_3 + C_4 - C_6 - C_8 - \frac{1}{2}C_9 - \frac{1}{2}C_{10}\right] \\
&-M^P_a\xi_t\left[C_5 - \frac{1}{2}C_7\right] \;+\; F_a\left[\xi_u\left(-C_1 - \frac{1}{3}C_2\right)\right. \\
&\left. -\xi_t\left(\frac{1}{3}C_3 + C_4 + \frac{3}{2}C_7 + \frac{1}{2}C_8 - \frac{5}{3}C_9 - C_{10}\right)\right] \\
&-F^P_a\xi_t\left[\frac{1}{3}C_5 + C_6 - \frac{1}{6}C_7 - \frac{1}{2}C_8\right]. \qquad (31)
\end{aligned}$$

The decay amplitude for $B^0 \to \pi^0\rho^0$ can be written as

$$\begin{aligned}
-2\mathcal{M}(B^0 \to \pi^0\rho^0) &= F_e\left[\xi_u\left(C_1 + \frac{1}{3}C_2\right)\right. \\
&\left. -\xi_t\left(-\frac{1}{3}C_3 - C_4 + \frac{3}{2}C_7 + \frac{1}{2}C_8 + \frac{5}{3}C_9 + C_{10}\right)\right] \\
&+F_{e\rho}\left[\xi_u\left(C_1 + \frac{1}{3}C_2\right)\right. \\
&\left. -\xi_t\left(-\frac{1}{3}C_3 - C_4 - \frac{3}{2}C_7 - \frac{1}{2}C_8 + \frac{5}{3}C_9 + C_{10}\right)\right] \\
&+F^P_{e\rho}\xi_t\left[\frac{1}{3}C_5 + C_6 - \frac{1}{6}C_7 - \frac{1}{2}C_8\right] \\
&+M_e\left[\xi_u C_2 - \xi_t\left(-C_3 - \frac{3}{2}C_8 + \frac{1}{2}C_9 + \frac{3}{2}C_{10}\right)\right] \\
&+M_{e\rho}\left[\xi_u C_2 - \xi_t\left(-C_3 + \frac{3}{2}C_8 + \frac{1}{2}C_9 + \frac{3}{2}C_{10}\right)\right] \\
&-(M_a + M_{a\rho})\left[\xi_u C_2\right. \\
&\left. - \xi_t\left(C_3 + 2C_4 - 2C_6 - \frac{1}{2}C_8 - \frac{1}{2}C_9 + \frac{1}{2}C_{10}\right)\right] \\
&+(M^P_e + 2M^P_a)\xi_t\left[C_5 - \frac{1}{2}C_7\right]. \qquad (32)
\end{aligned}$$

The decay amplitude for $B^+ \to \rho^+\pi^0$ can be written as

$$\begin{aligned}
\sqrt{2}\mathcal{M}(B^+ \to \rho^+\pi^0) &= (F_e + 2F_a)\left[\xi_u\left(\frac{1}{3}C_1 + C_2\right)\right. \\
&\left. -\xi_t\left(\frac{1}{3}C_3 + C_4 + C_{10} + \frac{1}{3}C_9\right)\right] \\
&+F_{e\rho}\left[\xi_u\left(C_1 + \frac{1}{3}C_2\right)\right. \\
&\left. - \xi_t\left(-\frac{1}{3}C_3 - C_4 - \frac{3}{2}C_7 - \frac{1}{2}C_8 + C_{10} + \frac{5}{3}C_9\right)\right] \\
&-F^P_{e\rho}\xi_t\left[-\frac{1}{3}C_5 - C_6 + \frac{1}{2}C_8 + \frac{1}{6}C_7\right] \\
&+M_{e\rho}\left[\xi_u C_2 - \xi_t\left(-C_3 + \frac{3}{2}C_8 + \frac{1}{2}C_9 + \frac{3}{2}C_{10}\right)\right] \\
&+(M_e + M_a - M_{a\rho})\left[\xi_u C_1 - \xi_t\left(C_3 + C_9\right)\right] \\
&-M^P_e\xi_t\left[C_5 + C_7\right] \\
&-2F^P_a\xi_t\left[\frac{1}{3}C_5 + C_6 + \frac{1}{3}C_7 + C_8\right]. \qquad (33)
\end{aligned}$$

The decay amplitude for $B^+ \to \pi^+\rho^0$ can be written as

$$\begin{aligned}
\sqrt{2}\mathcal{M}(B^+ \to \pi^+\rho^0) &= F_e\left[\xi_u\left(C_1 + \frac{1}{3}C_2\right)\right. \\
&\left. -\xi_t\left(-\frac{1}{3}C_3 - C_4 + \frac{3}{2}C_7 + \frac{1}{2}C_8 + \frac{5}{3}C_9 + C_{10}\right)\right] \\
&+(F_{e\rho} - 2F_a)\left[\xi_u\left(\frac{1}{3}C_1 + C_2\right)\right. \\
&\left. - \xi_t\left(\frac{1}{3}C_3 + C_4 + \frac{1}{3}C_9 + C_{10}\right)\right] \\
&-(F^P_{e\rho} - 2F^P_a)\xi_t\left[\frac{1}{3}C_5 + C_6 + \frac{1}{3}C_7 + C_8\right] \\
&+M_e\left[\xi_u C_2 - \xi_t\left(-C_3 - \frac{3}{2}C_8 + \frac{1}{2}C_9 + \frac{3}{2}C_{10}\right)\right] \\
&+(M_{e\rho} - M_a + M_{a\rho})\left[\xi_u C_1 - \xi_t(C_3 + C_9)\right] \\
&+M^P_e\xi_t\left[C_5 - \frac{1}{2}C_7\right]. \qquad (34)
\end{aligned}$$

From (30)–(34), we can verify that the isospin relation

$$\mathcal{M}(B^0 \to \pi^+\rho^-) + \mathcal{M}(B^0 \to \pi^-\rho^+) - 2\mathcal{M}(B^0 \to \pi^0\rho^0) = \sqrt{2}\mathcal{M}(B^+ \to \pi^0\rho^+) + \sqrt{2}\mathcal{M}(B^+ \to \pi^+\rho^0) \quad (35)$$

holds exactly in our calculations.

The decay amplitude for $B^+ \to \pi^+\omega$ can also be written as an expression of the above F_i and M_i, but one should remember replacing f_ρ by f_ω and ϕ_ρ by ϕ_ω

$$\begin{aligned}
&\sqrt{2}\mathcal{M}(B^+ \to \pi^+\omega)\\
&= F_e\left[\xi_u\left(C_1+\frac{1}{3}C_2\right) - \xi_t\left(\frac{7}{3}C_3+\frac{5}{3}C_4+2C_5+\frac{2}{3}C_6\right.\right.\\
&\left.\left.+\frac{1}{2}C_7+\frac{1}{6}C_8+\frac{1}{3}C_9-\frac{1}{3}C_{10}\right)\right]\\
&+ F_{e\rho}\left[\xi_u\left(\frac{1}{3}C_1+C_2\right) - \xi_t\left(\frac{1}{3}C_3+C_4+\frac{1}{3}C_9+C_{10}\right)\right]\\
&- F_{e\rho}^P\xi_t\left[\frac{1}{3}C_5+C_6+\frac{1}{3}C_7+C_8\right]\\
&+ M_e\left[\xi_u C_2 - \xi_t\left(C_3+2C_4-2C_6-\frac{1}{2}C_8\right.\right.\\
&\left.\left.-\frac{1}{2}C_9+\frac{1}{2}C_{10}\right)\right]\\
&+ (M_{e\rho}+M_a+M_{a\rho})\left[\xi_u C_1 - \xi_t\left(C_3+C_9\right)\right]\\
&- (M_a^P+M_{a\rho}^P)\xi_t\left[C_5+C_7\right] - M_e^P\xi_t\left[C_5-\frac{1}{2}C_7\right]. \quad (36)
\end{aligned}$$

The decay amplitude for $B^0 \to \pi^0\omega$ can be written as

$$\begin{aligned}
&2\mathcal{M}(B^0 \to \pi^0\omega) = F_e\left[\xi_u\left(-C_1-\frac{1}{3}C_2\right)\right.\\
&-\xi_t\left(-\frac{7}{3}C_3-\frac{5}{3}C_4-2C_5-\frac{2}{3}C_6-\frac{1}{2}C_7-\frac{1}{6}C_8\right.\\
&\left.\left.-\frac{1}{3}C_9+\frac{1}{3}C_{10}\right)\right] + F_{e\rho}\left[\xi_u\left(C_1+\frac{1}{3}C_2\right)\right.\\
&\left.-\xi_t\left(-\frac{1}{3}C_3-C_4-\frac{3}{2}C_7-\frac{1}{2}C_8+\frac{5}{3}C_9+C_{10}\right)\right]\\
&+F_{e\rho}^P\xi_t\left[C_6+\frac{1}{3}C_5-\frac{1}{6}C_7-\frac{1}{2}C_8\right]\\
&+M_e\left[-\xi_u C_2 - \xi_t\left(-C_3-2C_4+2C_6+\frac{1}{2}C_8\right.\right.\\
&\left.\left.+\frac{1}{2}C_9-\frac{1}{2}C_{10}\right)\right]\\
&+M_{e\rho}\left[\xi_u C_2 - \xi_t\left(-C_3+\frac{3}{2}C_8+\frac{1}{2}C_9+\frac{3}{2}C_{10}\right)\right]\\
&+(M_a+M_{a\rho})\left[\xi_u C_2 - \xi_t\left(-C_3-\frac{3}{2}C_8\right.\right.\\
&\left.\left.+\frac{1}{2}C_9+\frac{3}{2}C_{10}\right)\right]\\
&+(M_e^P+2M_a^P)\xi_t\left[C_5-\frac{1}{2}C_7\right]. \quad (37)
\end{aligned}$$

4 Numerical calculations and discussions of results

In the numerical calculations we use

$$\begin{aligned}
\Lambda_{\overline{\rm MS}}^{(f=4)} &= 0.25\,{\rm GeV}, \quad f_\pi = 130\,{\rm MeV},\\
f_B &= 190\,{\rm MeV},\\
m_0 &= 1.4\,{\rm GeV}, \quad f_\rho = f_\omega = 200\,{\rm MeV},\\
f_\rho^T &= f_\omega^T = 160\,{\rm MeV},\\
M_B &= 5.2792\,{\rm GeV}, \quad M_W = 80.41\,{\rm GeV}. \quad (38)
\end{aligned}$$

Note that for simplicity we use the same value for f_ρ (f_ρ^T) and f_ω (f_ω^T). This also makes it easy for us to see the major difference for the two mesons in B decays. In principle, the decay constants can be a little different. For the light meson wave function, we neglect the b dependent part, which is not important in the numerical analysis. We use the wave function for ϕ_π^A and the twist-3 wave functions ϕ_π^P and ϕ_π^t from [16]:

$$\begin{aligned}
\phi_\pi^A(x) &= \frac{3}{\sqrt{6}}f_\pi x(1-x) \quad (39)\\
&\times\left[1+0.44C_2^{3/2}(2x-1)+0.25C_4^{3/2}(2x-1)\right],\\
\phi_\pi^P(x) &= \frac{f_\pi}{2\sqrt{6}} \quad (40)\\
&\times\left[1+0.43C_2^{1/2}(2x-1)+0.09C_4^{1/2}(2x-1)\right],\\
\phi_\pi^t(x) &= \frac{f_\pi}{2\sqrt{6}}(1-2x)\left[1+0.55(10x^2-10x+1)\right]. \quad (41)
\end{aligned}$$

The Gegenbauer polynomials are defined by

$$\begin{aligned}
&C_2^{1/2}(t) = \frac{1}{2}(3t^2-1),\ C_4^{1/2}(t) = \frac{1}{8}(35t^4-30t^2+3),\\
&C_2^{3/2}(t) = \frac{3}{2}(5t^2-1),\ C_4^{3/2}(t) = \frac{15}{8}(21t^4-14t^2+1), \quad (42)
\end{aligned}$$

whose coefficients correspond to $m_0 = 1.4\,{\rm GeV}$. In the $B \to \pi\rho$, $\pi\omega$ decays, it is the longitudinal polarization of the ρ and ω-meson which contributes to the decay amplitude. Therefore we choose the wave function of the ρ- and ω-meson similar to the pion case in (39) and (41) [17]:

$$\begin{aligned}
\phi_\rho(x) &= \phi_\omega(x)\\
&= \frac{3}{\sqrt{6}}f_\rho x(1-x)\left[1+0.18C_2^{3/2}(2x-1)\right], \quad (43)\\
\phi_\rho^t(x) &= \phi_\omega^t(x)\\
&= \frac{f_\rho^T}{2\sqrt{6}}\Big\{3(2x-1)^2+0.3(2x-1)^2\\
&\times\left[5(2x-1)^2-3\right]\\
&+0.21[3-30(2x-1)^2+35(2x-1)^4]\Big\}, \quad (44)\\
\phi_\rho^s(x) &= \phi_\omega^s(x) \quad (45)\\
&= \frac{3}{2\sqrt{6}}f_\rho^T(1-2x)\left[1+0.76(10x^2-10x+1)\right].
\end{aligned}$$

Here, again for simplicity, we use the same expression for ρ- and ω-mesons.

For the B-meson, the wave function is chosen as

$$\phi_B(x,b) = \frac{N_B}{2\sqrt{6}} f_B x^2(1-x)^2 \times \exp\left[-\frac{M_B^2\, x^2}{2\omega_b^2} - \frac{1}{2}(\omega_b b)^2\right], \quad (46)$$

with $\omega_b = 0.4\,\mathrm{GeV}$. $N_B = 2365.57$ is a normalization factor. We include the full expression of the twist-3 wave functions for the light mesons, unlike $B \to \pi\pi$ decays [10]. The twist-3 wave functions are also adopted from QCD sum rule calculations [16]. These changes make the $B \to \rho$ form factor a little larger than the $B \to \pi$ form factor [13]. However, this set of parameters does not change the $B^0 \to \pi^+\pi^-$ branching ratios. We will see later that this set of parameters will give good results for $B \to \pi\rho$ and $\pi\omega$ decays. With the wave functions chosen above we get the corresponding form factors at zero momentum transfer from (13) and (23):

$$F_0^{B\to\pi} = 0.30, \quad A_0^{B\to\rho} = 0.37.$$

They are close to the light-cone QCD sum rule results [18].

The CKM parameters we used here are [19]

$$|V_{ud}| = 0.9735 \pm 0.0008, \quad |V_{ub}/V_{cb}| = 0.090 \pm 0.025,$$
$$|V_{cb}| = 0.0405 \pm 0.0019, \quad |V_{tb}^* V_{td}| = 0.0083 \pm 0.0016. \quad (47)$$

We leave the CKM angle ϕ_2 as a free parameter. The definition of ϕ_2 is

$$\phi_2 = \arg\left[-\frac{V_{td}V_{tb}^*}{V_{ud}V_{ub}^*}\right]. \quad (48)$$

In this parameterization, the decay amplitude of $B \to \pi\rho$ (or $\pi\omega$) can be rewritten as

$$\mathcal{M} = V_{ub}^* V_{ud} T - V_{tb}^* V_{td} P = V_{ub}^* V_{ud} T \left[1 + z\mathrm{e}^{\mathrm{i}(\phi_2+\delta)}\right], \quad (49)$$

where $z = |V_{tb}^* V_{td}/V_{ub}^* V_{ud}|\,|P/T|$, and δ is the relative strong phase between tree (T) diagrams and penguin diagrams (P). z and δ can be calculated from PQCD. The corresponding charge conjugate decay mode is then

$$\overline{\mathcal{M}} = V_{ub} V_{ud}^* T - V_{tb} V_{td}^* P = V_{ub} V_{ud}^* T \left[1 + z\mathrm{e}^{\mathrm{i}(-\phi_2+\delta)}\right]. \quad (50)$$

Therefore the averaged branching ratio for $B \to \pi\rho$ is

$$\mathrm{Br} = (|\mathcal{M}|^2 + |\overline{\mathcal{M}}|^2)/2 = |V_{ub}V_{ud}^* T|^2 \left[1 + 2z\cos\phi_2\cos\delta + z^2\right], \quad (51)$$

where $z = |V_{tb}V_{td}^*/V_{ub}V_{ud}^*|\,|P/T|$. Equation (51) shows that the averaged branching ratio is a function of $\cos\phi_2$.

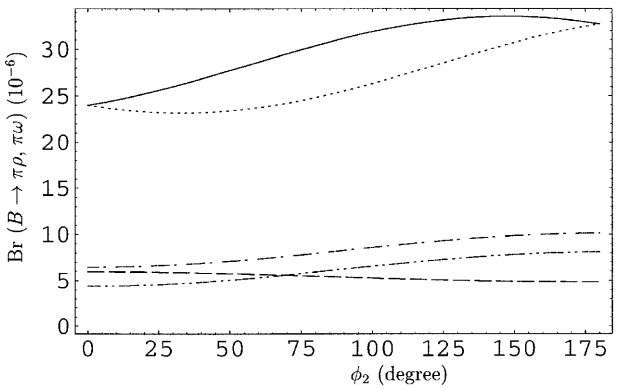

Fig. 3. Branching ratios (10^{-6}) of $B^0/\bar{B}^0 \to \pi^+\rho^-$ (solid line), $B^0/\bar{B}^0 \to \rho^+\pi^-$ (dotted line), $B^+ \to \pi^+\rho^0$ (dashed line), $B^+ \to \rho^+\pi^0$ (dash-dotted line), and $B^+ \to \pi^+\omega$ (dash-dotted-dotted line), as a function of CKM angle ϕ_2

This gives a potential method to determine the CKM angle ϕ_2 by measuring only the averaged non-leptonic decay branching ratios. In our PQCD approach, the branching ratios and also the other quantities in (51) are all calculable, so that $\cos\phi_2$ is measurable. However, there are still uncertainties in the input parameters of our approach as discussed below. More experimental data from BABAR and Belle can restrict these parameters in the near future.

A more complicated thing to consider is that there are four decay channels of $B^0/\bar{B}^0 \to \pi^+\rho^-$, $B^0/\bar{B}^0 \to \rho^+\pi^-$. Due to $B\bar{B}$ mixing, it is very difficult to distinguish B^0 from $\bar{B}^0$. But it is very easy to identify the final states. Therefore we sum up $B^0/\bar{B}^0 \to \pi^+\rho^-$ as one channel, and $B^0/\bar{B}^0 \to \rho^+\pi^-$ as another, although the summed up channels are not charge conjugate states. We show the branching ratio of $B^0/\bar{B}^0 \to \pi^+\rho^-$, $B^0/\bar{B}^0 \to \rho^+\pi^-$, $B^+ \to \pi^+\rho^0$, $B^+ \to \rho^+\pi^0$, and $B^+ \to \pi^+\omega$ decays as a function of ϕ_2 in Fig. 3. The branching ratio of $B^0/\bar{B}^0 \to \pi^+\rho^-$ is a little larger than that of the $B^0/\bar{B}^0 \to \pi^-\rho^+$ decays. Each of them is a sum of two decay channels. They all get larger when ϕ_2 is larger. The average of the two is in agreement with the recently measured branching ratios by CLEO [1] and BABAR [20]:

$$\mathrm{Br}(B^0 \to \pi^+\rho^- + \pi^-\rho^+) = 27.6^{+8.4}_{-7.4} \pm 4.2 \times 10^{-6}, \quad \text{CLEO}, \quad (52)$$

$$\mathrm{Br}(B^0 \to \pi^+\rho^- + \pi^-\rho^+) = 28.9 \pm 5.4 \pm 4.3 \times 10^{-6}, \quad \text{BABAR}. \quad (53)$$

There are still large uncertainties in the experimental results. Therefore it is still too early to fully determine the input parameters and to obtain the CKM angle ϕ_2 from experiments.

The most uncertain parameters in our approach concern the meson wave functions. In principle, they can only be restricted by experiments, namely, semi-leptonic and non-leptonic decays of B-mesons. Our parameters chosen for the numerical calculations in (38) and (46) are best fit values from $B \to \pi\pi$ decays [10], $B \to \pi K$ [14], $B \to \pi$, $B \to \rho$ semi-leptonic decays [13] and some other experiments. As in these decays, we show the ω_b dependence of

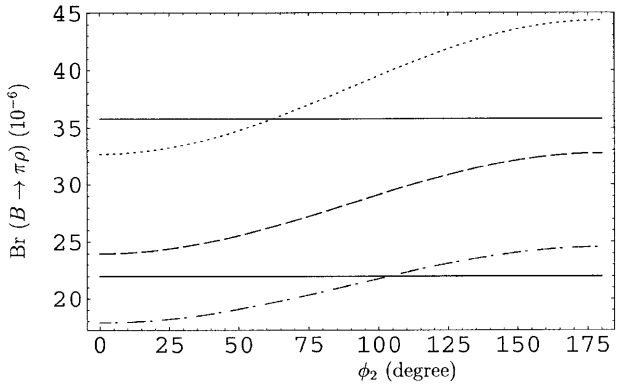

Fig. 4. Branching ratios of $B^0/\bar{B}^0 \to \pi^\pm\rho^\mp$ decays: $\omega_b = 0.36$ (dotted line), $\omega_b = 0.40$ (dashed line) and $\omega_b = 0.44$ (dash-dotted line) as a function of the CKM angle ϕ_2. The two horizontal lines are BABAR measurement limits

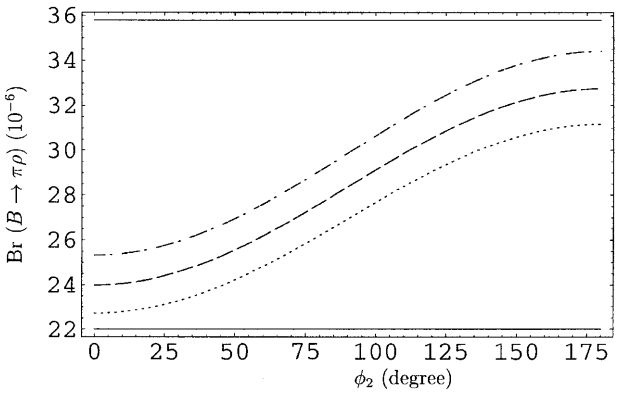

Fig. 5. Branching ratios of $B^0/\bar{B}^0 \to \pi^\pm\rho^\mp$ decays: $m_0 = 1.3\,\text{GeV}$ (dotted line), $m_0 = 1.4\,\text{GeV}$ (dashed line) and $m_0 = 1.5\,\text{GeV}$ (dash-dotted line) as a function of the CKM angle ϕ_2. The two horizontal lines are BABAR measurement limits

the branching ratios $\text{Br}(B^0/\bar{B}^0 \to \pi^\pm\rho^\mp)$ in Fig. 4. The dotted, dashed and dash-dotted lines are for $\omega_b = 0.36$, 0.40 and 0.44, respectively. They are also shown as a function of the CKM angle ϕ_2. The two horizontal lines in the figure are BABAR measurements of 1σ. From the figure, we can see that the branching ratio is quite sensitive to the ω_b parameter. Fortunately, this parameter is also restricted from semi-leptonic decays [13]. In the near future, it will not be a big problem.

In Fig. 5 we show the branching ratio of $B^0/\bar{B}^0 \to \pi^\pm\rho^\mp$ decays: $m_0 = 1.3\,\text{GeV}$ (dotted line), $m_0 = 1.4\,\text{GeV}$ (dashed line) and $m_0 = 1.5\,\text{GeV}$ (dash-dotted line) as a function of the CKM angle ϕ_2. m_0 is a parameter characterizing the relative size of the twist-3 contribution to the twist-2 contribution. It originates from chiral perturbation theory and has a value near 1 GeV. Because of the chiral enhancement of m_0, the twist-3 contribution is at the same order of magnitude as the twist-2 contribution. Thus the branching ratios of $\text{Br}(B^0/\bar{B}^0 \to \pi^\pm\rho^\mp)$ are also sensitive to this parameter, but not as strongly as the ω_b dependence.

The branching ratios of $B^+ \to \pi^+\rho^0$ and $B^+ \to \pi^+\omega$ have little dependence on ϕ_2. They are a little smaller than

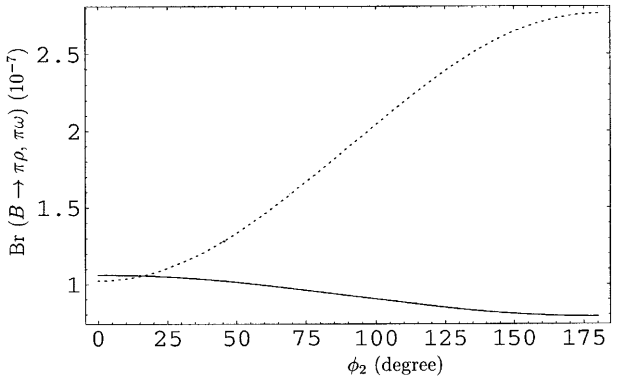

Fig. 6. Branching ratios (10^{-7}) of $B^0 \to \pi^0\rho^0$ (solid line), $B^0 \to \pi^0\omega$ (dotted line), as a function of CKM angle ϕ_2

the CLEO measurement [1] shown below, but still within experimental error bars. We have

$$\text{Br}(B^+ \to \pi^+\rho^0) = 10.4^{+3.3}_{-3.4} \pm 2.1 10^{-6}, \tag{54}$$

$$\text{Br}(B^+ \to \pi^+\omega) = 11.3^{+3.3}_{-2.9} \pm 1.4 10^{-6}. \tag{55}$$

However, the recent BABAR measurement is in good agreement with our prediction for $B^+ \to \pi^+\omega$ [21]:

$$\text{Br}(B^+ \to \pi^+\omega) = 6.6^{+2.1}_{-1.8} \pm 0.7 \times 10^{-6}, \tag{56}$$

where the error bars are also smaller. The preliminary result of Belle shows that the branching ratio of $B^+ \to \pi^+\rho^0$ is around 6×10^{-6} [22]. This agrees with our prediction in Fig. 3.

The averaged branching ratios of $B^0 \to \pi^0\rho^0$ and $\pi^0\omega$ are shown in Fig. 6. They also have a large dependence on ϕ_2. Their behavior is quite different, due to the different isospin of ρ^0 and ω. But their branching ratios are rather small, around 10^{-7}. They may not be measured in the current running B factories, but this may be possible in future experiments, like LHC-B and NLC. The recent BABAR upper limit of the channel is [20]

$$\text{Br}(B^0 \to \pi^0\rho^0) < 10.6 \times 10^{-6}. \tag{57}$$

This is still consistent with our predictions in the standard model (SM).

Using (49) and (50), we can derive the direct CP-violating parameter to find

$$A_{CP}^{\text{dir}} = \frac{|\mathcal{M}|^2 - |\overline{\mathcal{M}}|^2}{|\mathcal{M}|^2 + |\overline{\mathcal{M}}|^2} = \frac{2\sin\phi_2 \sin\delta}{1 + 2z\cos\phi_2\cos\delta + z^2}. \tag{58}$$

Unsurprisingly, it is a function of $\cos\phi_2$ and $\sin\phi_2$. It is calculable in our PQCD approach. The direct CP-violation parameters as a function of ϕ_2 are shown in Fig. 7. The direct CP-violation parameter of $B^+ \to \pi^+\rho^0$ and $B^0 \to \pi^0\rho^0$ are positive and very large, while the direct CP-violation parameter of $B^+ \to \rho^+\pi^0$ and $B^0 \to \pi^0\omega$ are negative and very large. The large strong phase required by the large direct CP-asymmetry is from the non-factorizable and annihilation type diagrams, especially the

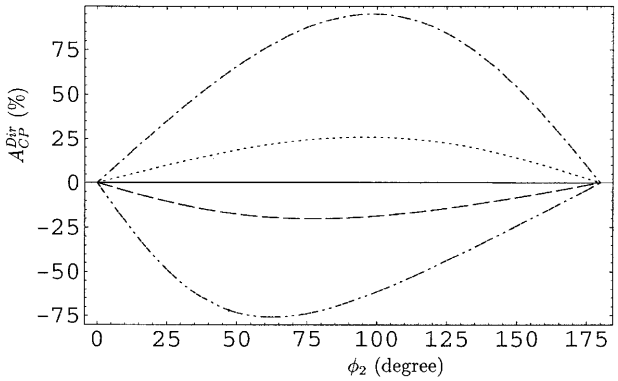

Fig. 7. Direct CP-violation parameters of $B^+ \to \pi^+\omega$ (solid line), $B^+ \to \pi^+\rho^0$ (dotted line), $B^+ \to \rho^+\pi^0$ (dashed line), $B^0 \to \rho^0\pi^0$ (dash-dotted line), $B^0 \to \pi^0\omega$ (dash-dotted-dotted line), as a function of the CKM angle ϕ_2

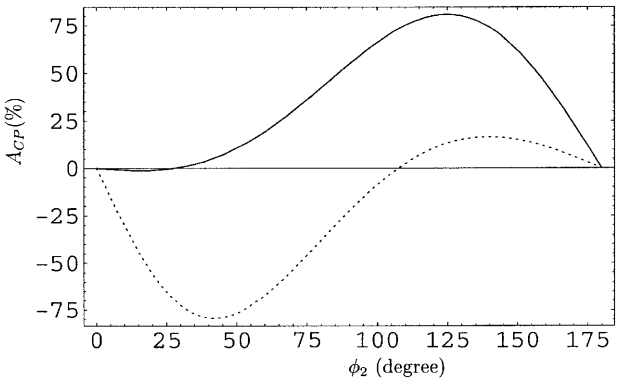

Fig. 8. Total CP-asymmetries of $B^0 \to \pi^0\rho^0$ (solid line), and $B^0 \to \pi^0\omega$ (dotted line), as a function of the CKM angle ϕ_2

annihilation diagrams. This is different from the situation in the factorization approach where the main contribution comes from the BSS mechanism [23] and the annihilation diagram has been neglected [24]. The direct CP-violation of $B^+ \to \pi^+\omega$ is rather small, since the annihilation diagram contributions in this decay is almost canceled in (36). The preliminary measurement of CLEO shows a large CP-asymmetry for this decay [25]:

$$A_{CP}(B^+ \to \pi^+\omega) = 34 \pm 25\%. \tag{59}$$

Although the sign of this CP asymmetry is in agreement with our prediction, the central value is too large. If the result of the central value remains in future experiments, we may expect new physics contributions.

For the neutral B^0 decays, there is a more complication situation because of the $B^0\overline{B^0}$ mixing. The CP-asymmetry is time dependent [24]:

$$A_{CP}(t) \simeq A_{CP}^{\rm dir}\cos(\Delta m t) + a_{\epsilon+\epsilon'}\sin(\Delta m t), \tag{60}$$

where Δm is the mass difference of the two mass eigenstates of the neutral B-meson. The direct CP-violation parameter $A_{CP}^{\rm dir}$ has already been defined in (58), while the mixing-related CP-violation parameter is defined by

$$a_{\epsilon+\epsilon'} = \frac{-2{\rm Im}(\lambda_{CP})}{1+|\lambda_{CP}|^2}, \tag{61}$$

where

$$\lambda_{CP} = \frac{V_{tb}^* V_{td}\langle f|H_{\rm eff}|\overline{B}^0\rangle}{V_{tb}V_{td}^*\langle f|H_{\rm eff}|B^0\rangle}. \tag{62}$$

Using (49) and (50), we can derive

$$\lambda_{CP} = {\rm e}^{2{\rm i}\phi_2}\frac{1+z{\rm e}^{{\rm i}(\delta-\phi_2)}}{1+z{\rm e}^{{\rm i}(\delta+\phi_2)}}. \tag{63}$$

λ_{CP} and $a_{\epsilon+\epsilon'}$ are functions of the CKM angle ϕ_2 only. Therefore, the CP-asymmetry of $B \to \pi\rho$ and $\pi\omega$ decays can measure the CKM angle ϕ_2, even if for the neutral B decays including the $B\bar{B}$ mixing effect.

If we integrate over the time variable t, we will get the total CP-asymmetry

$$A_{CP} = \frac{1}{1+x^2}A_{CP}^{\rm dir} + \frac{x}{1+x^2}a_{\epsilon+\epsilon'}, \tag{64}$$

with $x = \Delta m/\Gamma \simeq 0.723$ for the $B^0\overline{B}^0$ mixing in the SM [19]. The total CP-asymmetries of $B^0 \to \pi^0\rho^0$, $\pi^0\omega$ are shown in Fig. 8. Although the CP-asymmetries are large, it is still difficult to measure them, since their branching ratios are small, around 10^{-7}.

The CP-asymmetries of $B^0/\bar{B}^0 \to \pi^\pm\rho^\mp$ are very complicated. Here one studies the four time-dependent decay widths for $B^0(t) \to \pi^+\rho^-$, $\bar{B}^0(t) \to \pi^-\rho^+$, $B^0(t) \to \pi^-\rho^+$ and $\bar{B}^0(t) \to \pi^+\rho^-$ [26–28]. These time-dependent widths can be expressed by four basic matrix elements:

$$\begin{aligned} &g = \langle\pi^+\rho^-|H_{\rm eff}|B^0\rangle,\ h = \langle\pi^+\rho^-|H_{\rm eff}|\bar{B}^0\rangle,\\ &\bar{g} = \langle\pi^-\rho^+|H_{\rm eff}|\bar{B}^0\rangle,\ \bar{h} = \langle\pi^-\rho^+|H_{\rm eff}|B^0\rangle, \end{aligned} \tag{65}$$

which determine the decay matrix elements of $B^0 \to \pi^+\rho^-$ and $\pi^-\rho^+$, and of $\bar{B}^0 \to \pi^-\rho^+$ and $\pi^+\rho^-$ at $t = 0$. The matrix elements g and $\bar{h}$ are given in (30) and (31). The matrix elements h and $\bar{g}$ are obtained from $\bar{h}$ and g by changing the signs of the weak phases contained in the products of the CKM matrix elements. We also need to know the CP-violating parameter coming from the $B^0\bar{B}^0$ mixing. Defining

$$\begin{aligned} B_1 &= p|B^0\rangle + q|\bar{B}^0\rangle,\\ B_2 &= p|B^0\rangle - q|\bar{B}^0\rangle, \end{aligned} \tag{66}$$

with $|p|^2 + |q|^2 = 1$ and $q/p = (H_{21}/H_{12})^{1/2}$, with $H_{ij} = M_{ij} - {\rm i}/2\Gamma_{ij}$ representing the $|\Delta B| = 2$ and $\Delta Q = 0$ Hamiltonian. For the decays of B^0 and $\bar{B}^0$ we use

$$\frac{q}{p} = \frac{V_{tb}^* V_{td}}{V_{tb}V_{td}^*} = {\rm e}^{-2{\rm i}\phi_1}. \tag{67}$$

So $|q/p| = 1$ and this ratio has only a phase given by $-2\phi_1$. Then, the four time-dependent widths are given by the following formulae (we follow the notation of [28]):

$$\Gamma(B^0(t) \to \pi^+\rho^-) = {\rm e}^{-\Gamma t}\frac{1}{2}(|g|^2 + |h|^2)$$

$$\times \{1 + a_{\epsilon'} \cos \Delta mt + a_{\epsilon+\epsilon'} \sin \Delta mt\},$$
$$\Gamma(\bar{B}^0(t) \to \pi^- \rho^+) = \mathrm{e}^{-\Gamma t} \frac{1}{2}(|\bar{g}|^2 + |\bar{h}|^2)$$
$$\times \{1 - a_{\bar{\epsilon}'} \cos \Delta mt - a_{\epsilon+\bar{\epsilon}'} \sin \Delta mt\},$$
$$\Gamma(B^0(t) \to \pi^- \rho^+) = \mathrm{e}^{-\Gamma t} \frac{1}{2}(|\bar{g}|^2 + |\bar{h}|^2)$$
$$\times \{1 + a_{\bar{\epsilon}'} \cos \Delta mt + a_{\epsilon+\bar{\epsilon}'} \sin \Delta mt\},$$
$$\Gamma(\bar{B}^0(t) \to \pi^+ \rho^-) = \mathrm{e}^{-\Gamma t} \frac{1}{2}(|g|^2 + |h|^2)$$
$$\times \{1 - a_{\epsilon'} \cos \Delta mt - a_{\epsilon+\epsilon'} \sin \Delta mt\}, \quad (68)$$

where

$$a_{\epsilon'} = \frac{|g|^2 - |h|^2}{|g|^2 + |h|^2}, \qquad a_{\epsilon+\epsilon'} = \frac{-2\mathrm{Im}\left(\frac{q}{p}\frac{h}{g}\right)}{1 + |h/g|^2},$$
$$a_{\bar{\epsilon}'} = \frac{|\bar{h}|^2 - |\bar{g}|^2}{|\bar{h}|^2 + |\bar{g}|^2}, \qquad a_{\epsilon+\bar{\epsilon}'} = \frac{-2\mathrm{Im}\left(\frac{q}{p}\frac{\bar{g}}{\bar{h}}\right)}{1 + |\bar{g}/\bar{h}|^2}. \quad (69)$$

We calculate the above four CP-violation parameters related to $B^0/\bar{B}^0 \to \pi^\pm\rho^\mp$ decays in PQCD. The results are shown in Fig. 9 as a function of ϕ_2. Comparing the results with the factorization approach [24], we found that our predicted sizes of $a_{\epsilon'}$ and $a_{\bar{\epsilon}'}$ are smaller while $a_{\epsilon+\epsilon'}$ and $a_{\epsilon+\bar{\epsilon}'}$ are larger. By measuring the time-dependent spectrum of the decay rates of B^0 and $\bar{B}^0$, one can find the coefficients of the two functions $\cos \Delta mt$ and $\sin \Delta mt$ in (68) and extract the quantities $a_{\epsilon'}$, $a_{\epsilon+\epsilon'}$, $a_{\bar{\epsilon}'}$, and $a_{\epsilon+\bar{\epsilon}'}$. Using these experimental results, we can obtain the size of the CKM angle ϕ_2 from Fig. 9.

5 Summary

We calculated the $B^0 \to \pi^+\rho^-$, $B^0 \to \rho^+\pi^-$, $B^+ \to \rho^+\pi^0$, $B^+ \to \pi^+\rho^0$, $B^0 \to \pi^0\rho^0$, $B^+ \to \pi^+\omega$ and $B^0 \to \pi^0\omega$ decays, together with their charge conjugate modes, in a perturbative QCD approach. We calculated the $B \to \pi$ and $B \to \rho$ form factors, which are in agreement with the QCD sum rule calculations. In addition to the usual factorization contributions, we also calculated the non-factorizable and annihilation diagrams. Although these are sub-leading contributions in the branching ratios of these decays, they are not negligible. Furthermore these diagrams provide the necessary strong phases required by the direct CP-asymmetry measurement.

Our calculation gives the right branching ratios, which agrees well with the CLEO and BABAR measurements. We also predict large direct CP-asymmetries in the $B^+ \to \rho^+\pi^0$ and $B^+ \to \pi^+\rho^0$ decays. Including the $B\bar{B}$ mixing effect, the CP-asymmetries of $B^0 \to \pi^0\omega$ and $B^0 \to \pi^0\rho^0$ are very large, but their branching ratios are small in the SM. The CP-asymmetry parameters of the $B^0 \to \pi^+\rho^-$ and $B^0 \to \rho^+\pi^-$ decays require the time-dependent measurement of the branching ratios.

Acknowledgements. We thank our PQCD group members: Y.Y. Keum, E. Kou, T. Kurimoto, H.N. Li, T. Morozumi, A.I. Sanda, N. Sinha, R. Sinha, K. Ukai and T. Yoshikawa for helpful discussions. This work was supported by the Grant-in-Aid for Scientific Research on Priority Areas (Physics of CP-violation). We also thank JSPS for support.

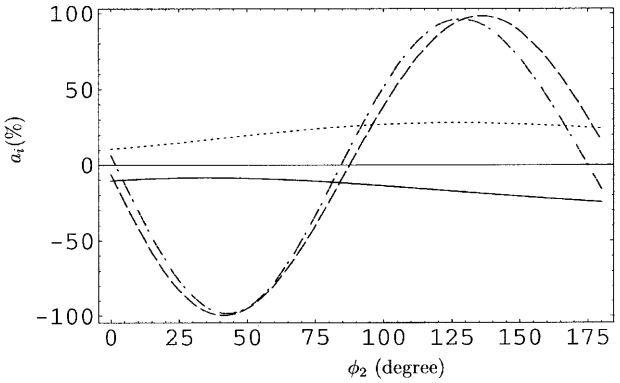

Fig. 9. CP-violation parameters of $B^0/\bar{B}^0 \to \pi^\pm\rho^\mp$ decays: $a_{\epsilon'}$(solid line), $a_{\bar{\epsilon}'}$ (dotted line), $a_{\epsilon+\epsilon'}$ (dashed line) and $a_{\epsilon+\bar{\epsilon}'}$ (dash-dotted line) as a function of CKM angle ϕ_2

Appendix

A Related functions defined in the text

We show here the functions h_i, coming from the Fourier transform of $H^{(0)}$,

$$h_e(x_1, x_2, b_1, b_2) = K_0\left(\sqrt{x_1 x_2} m_B b_1\right)$$
$$\times \Big[\theta(b_1 - b_2) K_0\left(\sqrt{x_2} m_B b_1\right) I_0\left(\sqrt{x_2} m_B b_2\right)$$
$$+\theta(b_2 - b_1) K_0\left(\sqrt{x_2} m_B b_2\right) I_0\left(\sqrt{x_2} m_B b_1\right)\Big] S_t(x_2), \quad (70)$$

$$h_d(x_1, x_2, x_3, b_1, b_2) = \alpha_s(t_d) K_0\left(-\mathrm{i}\sqrt{x_2 x_3} m_B b_2\right)$$
$$\times \Big[\theta(b_1 - b_2) K_0\left(\sqrt{x_1 x_2} m_B b_1\right) I_0\left(\sqrt{x_1 x_2} m_B b_2\right)$$
$$+\theta(b_2 - b_1) K_0\left(\sqrt{x_1 x_2} m_B b_2\right) I_0\left(\sqrt{x_1 x_2} m_B b_1\right)\Big], \quad (71)$$

$$h_f^1(x_1, x_2, x_3, b_1, b_2) = K_0\left(-\mathrm{i}\sqrt{x_2 x_3} m_B b_1\right) \alpha_s(t_f^1)$$
$$\times \Big[\theta(b_1 - b_2) K_0\left(-\mathrm{i}\sqrt{x_2 x_3} m_B b_1\right) J_0\left(\sqrt{x_2 x_3} m_B b_2\right)$$
$$+\theta(b_2 - b_1) K_0\left(-\mathrm{i}\sqrt{x_2 x_3} m_B b_2\right) J_0\left(\sqrt{x_2 x_3} m_B b_1\right)\Big], \quad (72)$$

$$h_f^2(x_1, x_2, x_3, b_1, b_2)$$
$$= K_0\left(\sqrt{x_2 + x_3 - x_2 x_3} m_B b_1\right) \alpha_s(t_f^2)$$
$$\times \Big[\theta(b_1 - b_2) K_0\left(-\mathrm{i}\sqrt{x_2 x_3} m_B b_1\right) J_0\left(\sqrt{x_2 x_3} m_B b_2\right)$$
$$+\theta(b_2 - b_1) K_0\left(-\mathrm{i}\sqrt{x_2 x_3} m_B b_2\right) J_0\left(\sqrt{x_2 x_3} m_B b_1\right)\Big], \quad (73)$$

$$h_a(x_1, x_2, b_1, b_2) = K_0\left(-\mathrm{i}\sqrt{x_1 x_2} m_B b_2\right) S_t(x_1)$$
$$\times \Big[\theta(b_1 - b_2) K_0\left(-\mathrm{i}\sqrt{x_1} m_B b_1\right) J_0\left(\sqrt{x_1} m_B b_2\right)$$

$$+\theta(b_2-b_1)K_0\left(-\mathrm{i}\sqrt{x_1}m_B b_2\right)J_0\left(\sqrt{x_1}m_B b_1\right)\Big], \quad (74)$$

where J_0 is the Bessel function and K_0, I_0 are modified Bessel functions with $K_0(-\mathrm{i}x) = -(\pi/2)Y_0(x) + \mathrm{i}(\pi/2)J_0(x)$. The threshold resummation form factor $S_t(x_i)$ is adopted from [13]:

$$S_t(x) = \frac{2^{1+2c}\Gamma(3/2+c)}{\sqrt{\pi}\Gamma(1+c)}[x(1-x)]^c, \quad (75)$$

where the parameter $c = 0.3$. This function is normalized to unity.

The Sudakov factors used in the text are defined by

$$\begin{aligned} S_{ab}(t) &= s\left(x_1 m_B/\sqrt{2}, b_1\right) + s\left(x_2 m_B/\sqrt{2}, b_2\right) \\ &+ s\left((1-x_2)m_B/\sqrt{2}, b_2\right) \\ &- \frac{1}{\beta_1}\left[\ln\frac{\ln(t/\Lambda)}{-\ln(b_1\Lambda)} + \ln\frac{\ln(t/\Lambda)}{-\ln(b_2\Lambda)}\right], \quad (76) \\ S_{cd}(t) &= s\left(x_1 m_B/\sqrt{2}, b_1\right) + s\left(x_2 m_B/\sqrt{2}, b_2\right) \\ &+ s\left((1-x_2)m_B/\sqrt{2}, b_2\right) \\ &+ s\left(x_3 m_B/\sqrt{2}, b_1\right) + s\left((1-x_3)m_B/\sqrt{2}, b_1\right) \\ &- \frac{1}{\beta_1}\left[2\ln\frac{\ln(t/\Lambda)}{-\ln(b_1\Lambda)} + \ln\frac{\ln(t/\Lambda)}{-\ln(b_2\Lambda)}\right], \quad (77) \\ S_{ef}(t) &= s\left(x_1 m_B/\sqrt{2}, b_1\right) + s\left(x_2 m_B/\sqrt{2}, b_2\right) \\ &+ s\left((1-x_2)m_B/\sqrt{2}, b_2\right) \\ &+ s\left(x_3 m_B/\sqrt{2}, b_2\right) + s\left((1-x_3)m_B/\sqrt{2}, b_2\right) \\ &- \frac{1}{\beta_1}\left[\ln\frac{\ln(t/\Lambda)}{-\ln(b_1\Lambda)} + 2\ln\frac{\ln(t/\Lambda)}{-\ln(b_2\Lambda)}\right], \quad (78) \\ S_{gh}(t) &= s\left(x_2 m_B/\sqrt{2}, b_1\right) + s\left(x_3 m_B/\sqrt{2}, b_2\right) \\ &+ s\left((1-x_2)m_B/\sqrt{2}, b_1\right) \\ &+ s\left((1-x_3)m_B/\sqrt{2}, b_2\right) \\ &- \frac{1}{\beta_1}\left[\ln\frac{\ln(t/\Lambda)}{-\ln(b_1\Lambda)} + \ln\frac{\ln(t/\Lambda)}{-\ln(b_2\Lambda)}\right], \quad (79) \end{aligned}$$

where the functions $s(q,b)$ are defined in Appendix A of [10]. The scales t_i in the above equations are chosen as

$$\begin{aligned} t_e^1 &= \max(\sqrt{x_2}m_B, 1/b_1, 1/b_2), \quad (80) \\ t_e^2 &= \max(\sqrt{x_1}m_B, 1/b_1, 1/b_2), \quad (81) \\ t_d &= \max(\sqrt{x_1x_2}m_B, \sqrt{x_2x_3}m_B, 1/b_1, 1/b_2), \quad (82) \\ t_f^1 &= \max(\sqrt{x_2x_3}m_B, 1/b_1, 1/b_2), \quad (83) \\ t_f^2 &= \max(\sqrt{x_2x_3}m_B, \sqrt{x_2+x_3-x_2x_3}m_B, 1/b_1, 1/b_2). \quad (84) \end{aligned}$$

References

1. A. Gritsan et al., CLEO Collaboration, talk at Lake Louis Winter Institute, February 20–26, 2000
2. H.R. Quinn, J.P. Silva, preprint hep-ph/0001290; A. Deandrea et al., preprint hep-ph/0002038; M.Z. Yang, Y.D. Yang, Phys. Rev. D **62**, 114019 (2000); D. Atwood, A. Soni, Phys. Lett. B **516**, 39 (2001)
3. D.S. Du, Z.Z. Xing, Phys. Rev. D **48**, 4155 (1993); G. Kramer, W.F. Palmer, H. Simma, Z. Phys. C **66**, 429 (1995); A. Ali, G. Kramer, C.D. Lü, Phys. Rev. D **58**, 094009 (1998); C.D. Lü, Nucl. Phys. Proc. Suppl. **74**, 227 (1999)
4. Y.-H. Chen, H.-Y. Cheng, B. Tseng, K.-C. Yang, Phys. Rev. D **60**, 094014 (1999)
5. C.H. Chang, H.N. Li, Phys. Rev. D **55**, 5577 (1997); T.W. Yeh, H.N. Li, Phys. Rev. D **56**, 1615 (1997)
6. H.N. Li, H.L. Yu, Phys. Rev. Lett. **74**, 4388 (1995); Phys. Lett. B **353**, 301 (1995); Phys. Rev. D **53**, 2486 (1996)
7. H.N. Li, Phys. Rev. D **52**, 3958 (1995)
8. H.N. Li, hep-ph/0102013
9. For a review, see G. Buchalla, A.J. Buras, M.E. Lautenbacher, Rev. Mod. Phys. **68**, 1125 (1996)
10. C.D. Lü, K. Ukai, M.Z. Yang, Phys. Rev. D **63**, 074009 (2001)
11. A.G. Grozin, M. Neubert, Phys. Rev. D **55**, 272 (1997); M. Beneke, T. Feldmann, Nucl. Phys. B **592**, 3 (2001)
12. M. Beneke, G. Buchalla, M. Neubert, C.T. Sachrajda, Nucl. Phys. B **591**, 313 (2000)
13. T. Kurimoto, H.-n. Li, A.I. Sanda, hep-ph/0105003
14. Y.Y. Keum, H.-n. Li, A.I. Sanda, Phys. Lett. B **504**, 6 (2001); Phys. Rev. D **63**, 054008 (2001); C.-h. Chen, H.-n. Li, Phys. Rev. D **63**, 014003 (2000)
15. For example, see: M. Beneke, G. Buchalla, M. Neubert, C.T. Sachrajda, Phys. Rev. Lett. **83**, 1914 (1999); Dongsheng Du, De-shan Yang, Guo-huai Zhu, Phys. Rev. D **64**, 014036 (2001); Hai-Yang Cheng, Kwei-Chou Yang, Phys. Rev. D **63**, 074011 (2001); Mao-Zhi Yang, Ya-Dong Yang, Phys. Rev. D **62**, 114019 (2000)
16. V.M. Braun, I.E. Filyanov, Z. Phys. C **48**, 239 (1990); P. Ball, J. High Energy Phys. **01**, 010 (1999)
17. P. Ball, V.M. Braun, Y. Koike, K. Tanaka, Nucl. Phys. B **529**, 323 (1998)
18. P. Ball, V.M. Braun, Phys. Rev. D **58**, 094016 (1998); P. Ball, J. High Energy Phys. **9809**, 005 (1998)
19. Particle Data Group, Eur. Phys. J. C **15**, 1 (2000)
20. B. Aubert et al., BABAR Collaboration, hep-ex/0107058
21. B. Aubert et al., BABAR Collaboration, hep-ex/0108017
22. P. Chang, talk given at International Europhysics Conference On High-Energy Physics, 12–18 July, 2001, Budapest, Hungary; private comunication
23. M. Bander, D. Silverman, A. Soni, Phys. Rev. Lett. **43**, 242 (1979)
24. A. Ali, G. Kramer, C.D. Lü, Phys. Rev. D **59**, 014005 (1999)
25. S. Chen et al., CELO Collaboration, hep-ex/0001009
26. M. Gronau, Phys. Lett. B **233**, 479 (1989)
27. R. Aleksan, I. Dunietz, B. Kayser, F. Le Diberder, Nucl. Phys. B **361**, 141 (1991)
28. W.F. Palmer, Y.L. Wu, Phys. Lett. B **350**, 245 (1995)